Dose-dependent induction of distinct phenotypic responses to Notch pathway activation in mammary epithelial cells

Marco Mazzone[a,1], Laura M. Selfors[a], John Albeck[a], Michael Overholtzer[b], Sanja Sale[a], Danielle L. Carroll[a,2], Darshan Pandya[a], Yiling Lu[c], Gordon B. Mills[c], Jon C. Aster[d], Spyros Artavanis-Tsakonas[a], and Joan S. Brugge[a,3]

[a]Department of Cell Biology, Harvard Medical School, Boston, MA 02115; [b]Cell Biology Program, Memorial Sloan-Kettering Cancer Center, New York, NY 10065; [c]Department of Systems Biology, The University of Texas M. D. Anderson Cancer Center, Houston, TX 77030; and [d]Department of Pathology, Brigham and Women's Hospital, Boston, MA 02115

Contributed by Joan S. Brugge, January 22, 2010 (sent for review December 3, 2009)

Aberrant activation of Notch receptors has been implicated in breast cancer; however, the mechanisms contributing to Notch-dependent transformation remain elusive because Notch displays dichotomous functional activities, promoting both proliferation and growth arrest. We investigated the cellular basis for the heterogeneous responses to Notch pathway activation in 3D cultures of MCF-10A mammary epithelial cells. Expression of a constitutively active Notch-1 intracellular domain (NICD) was found to induce two distinct types of 3D structures: large, hyperproliferative structures and small, growth-arrested structures with reduced cell-to-matrix adhesion. Interestingly, we found that these heterogeneous phenotypes reflect differences in Notch pathway activation levels; high Notch activity caused down-regulation of multiple matrix-adhesion genes and inhibition of proliferation, whereas low Notch activity maintained matrix adhesion and provoked a strong hyperproliferative response. Moreover, microarray analyses implicated NICD-induced p63 down-regulation in loss of matrix adhesion. In addition, a reverse-phase protein array-based analysis and subsequent loss-of-function studies identified STAT3 as a dominant downstream mediator of the NICD-induced outgrowth. These results indicate that the phenotypic responses to Notch are determined by the dose of pathway activation; and this dose affects the balance between growth-stimulative and growth-suppressive effects. This unique feature of Notch signaling provides insights into mechanisms that contribute to the dichotomous effects of Notch during development and tumorigenesis.

adhesion | breast | matrix | morphogenesis | transformation

Notch family receptors control evolutionarily conserved intercellular signaling pathways that regulate interactions between physically adjacent cells (1). Notch receptors play a role in a variety of developmental processes by controlling many diverse processes including proliferation, differentiation, and apoptosis (2). The biological effects of Notch are mediated through interactions with plasma membrane-associated ligands expressed on adjacent cells. After ligand binding, Notch is subjected to proteolytic cleavages that release the Notch intracellular domain (NICD), which moves to the nucleus where it participates in a transcriptional complex to regulate Notch-dependent gene expression (3).

Alterations of Notch pathway activity are associated with several human cancers (4). Most notably, alterations are linked to T-cell acute lymphoblastic leukemia, in which activating mutations within Notch-1 have been identified in >50% of tumors (5). Multiple lines of evidence implicate Notch receptors in breast cancer. Numb, a negative regulator of Notch pathway, is lost in >50% of human breast tumors through ubiquitination and proteasomal degradation, and its levels are inversely correlated with grade and proliferation rate (6). Furthermore, NICD is accumulated in a wide variety of human breast cancer cell lines, and elevated levels of Notch-1 and Jagged-1 mRNA in patients with breast cancer correlate with poor prognosis (7, 8). Within the murine mammary gland, transgenic expression of the activated form of Notch-1 or Notch-4 has been shown to provoke tumorigenesis (9, 10). In addition, both activated isoforms can transform normal murine and human mammary epithelial cells in soft-agar colony formation assays (11, 12).

The cellular mechanisms responsible for Notch-induced mammary tumorigenesis and dichotomous biological activities are not well understood. For this reason, we have examined the effects of NICD in 3D reconstituted basement membrane cultures of MCF-10A human mammary epithelial cells. Such cultures allow cells to organize into acinar structures that resemble the organization of mammary epithelial cells in vivo and consequently make it feasible to investigate morphogenetic activities of oncogenes that cannot be monitored in monolayer cultures (e.g., their ability to allow survival of cells in the luminal space, to disrupt cell–cell adhesion, their polarity, and other phenotypic effects) (13, 14). The most attractive aspect of these cultures is that it is possible to follow the fate of individual cells, because each acinus is generated by clonal outgrowth. Our studies revealed dramatic dose-dependent effects of Notch activation. Higher doses of Notch activity caused suppression of cell proliferation and clonal outgrowth, loss of ECM components and receptors, detachment of cells from ECM, and induction of cell-in-cell structures. Lower doses of Notch activity led to the generation of large colonies in soft agar and hyperproliferative acinar structures that maintain matrix adhesion. These results indicate that Notch pathway can induce heterogeneous phenotypes in mammary epithelial cells mainly through dose-dependent effects on matrix adhesion and cell proliferation.

Results

NICD Induces Heterogeneous Phenotypes in 3D Cultures of Mammary Epithelial Cells. To investigate the phenotypic changes induced by Notch pathway activation in mammary epithelial cells, we infected immortalized but nontumorigenic human MCF-10A cells with retroviral vectors that induce expression of either a drug-selectable marker alone (pBABE) or this marker together with constitutively active NICD. Stably infected MCF-10A cells overexpressing NICD were seeded in reconstituted basement membrane gels (Matrigel). As previously shown (15), MCF-10A cells grown in Matrigel form acinar-like 3D structures consisting of an outer layer of polarized, growth-arrested epithelial cells surrounding a hollow lumen and

Author contributions: M.M., G.B.M., S.A.T., and J.S.B. designed research; M.M., J.A., M.O., D.L.C., D.P., and Y.L. performed research; S.S., and J.C.A. contributed new reagents/analytic tools; M.M. and L.M.S. analyzed data; and M.M. and J.S.B. wrote the paper.

The authors declare no conflict of interest.

Freely available online through the PNAS open access option.

[1]Present address: Department of Experimental Oncology, European Institute of Oncology, Milan, 20139 Italy.

[2]Present address: Oncology Biology, Medimmune, Granta Park, Cambridge, CB1 6GH United Kingdom.

[3]To whom correspondence should be addressed. E-mail: joan_brugge@hms.harvard.edu.

This article contains supporting information online at www.pnas.org/cgi/content/full/1000896107/DCSupplemental.

with a basal deposition of basement membrane components such as laminins and collagens (see structures induced by pBABE in Fig. 1*A*). Strikingly, ≈10–20% of MCF-10A cells overexpressing NICD formed abnormal, noninvasive, hyperproliferative structures that were much larger than control structures (Fig. 1 *A* and *B*). Formation of these structures was dependent on exogenous EGF, and EGF-deficient medium did not support proliferation of either pBABE- or NICD-infected cells (Fig. 1*A, Insets*), in contrast to the EGF-independent phenotypes of MCF-10A cells expressing ErbB2, IGF-1R, PIK3CA mutants, or V-12Ras (14). The majority of cells overexpressing NICD failed to initiate proliferation or formed small structures with a highly aberrant morphology (black arrows in Fig. 1*A*), indicating that NICD overexpression interferes with the outgrowth of most MCF-10A acinar structures. For the sake of reference, we term these growth-inhibited structures "abortive."

Analysis of the NICD-induced structures at higher magnification by confocal microscopy using immunofluorescent markers that delineated cell membranes and nuclei revealed that many of the abortive structures were composed of large cells that contain internalized cells, reminiscent of previously described cell-in-cell structures (white arrows in Fig. 1*A*). Such structures are formed by the invasion of one cell into another by a process we previously referred to as "entosis" (16, 17). This process takes place following loss of matrix adhesion in a wide variety of normal and tumor cell lines in vitro and is commonly detected in nonadherent human tumor cells within fluid exudates (e.g., ascites, pleural fluid).

The detection of cell-in-cell structures in the 3D cultures suggested that NICD might induce loss of matrix adhesion. Indeed, NICD previously was found to cause detachment in both primary human mammary epithelial cells (18) and mouse mammary tumors (19). Accordingly, we found that MCF-10A cells transduced with a NICD retrovirus undergo a dramatic cell-detachment phenotype when replated shortly after infection and display cell-in-cell structures both in suspended and attached cells (Fig. 2*A*). In addition, NICD-infected cells also display reduced adhesion to

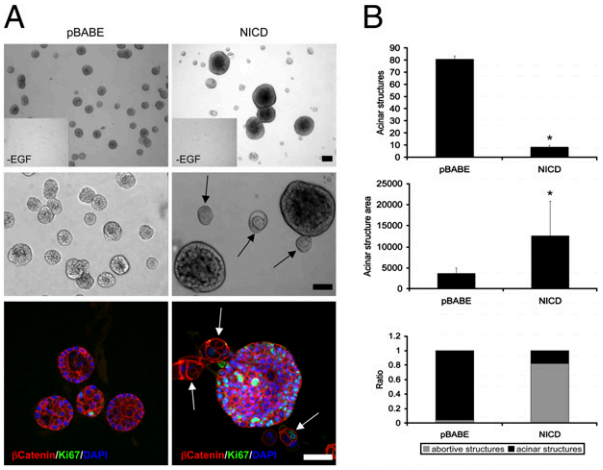

Fig. 1. NICD induces heterogeneous phenotypes in 3D cultures of mammary epithelial cells. (*A*) Control (pBABE) or NICD-overexpressing (NICD) MCF-10A cells were cultured in Matrigel for 2 weeks. The phase-contrast images show representative 3D structures. (Scale bars, 100 μm.) *Inserts* show the absence of 3D structures from cells cultured in absence of EGF. (*Bottom panels*) The fluorescent confocal microscopy images show staining for βcatenin (red), Ki67 (green), and DAPI (blue). The arrows indicate representative abortive 3D structures. (Scale bar, 100 μm.) (*B*) (*Top*) Data represent the mean number of counted acinar 3D structures. Error bars show ± SD of three replicate samples from one representative experiment. Two fields were counted together per sample. *, $P < 0.001$ relative to control. (*Middle*) The mean acinar structure area data are represented as pixel^2 and were obtained using ImageJ software. Error bars show ± SD of three replicate samples from one representative experiment. At least five fields were counted for sample. *, $P < 0.01$ relative to control. (*Bottom*) Ratio of the number of acinar structures or abortive structures relative to the total number of 3D structures.

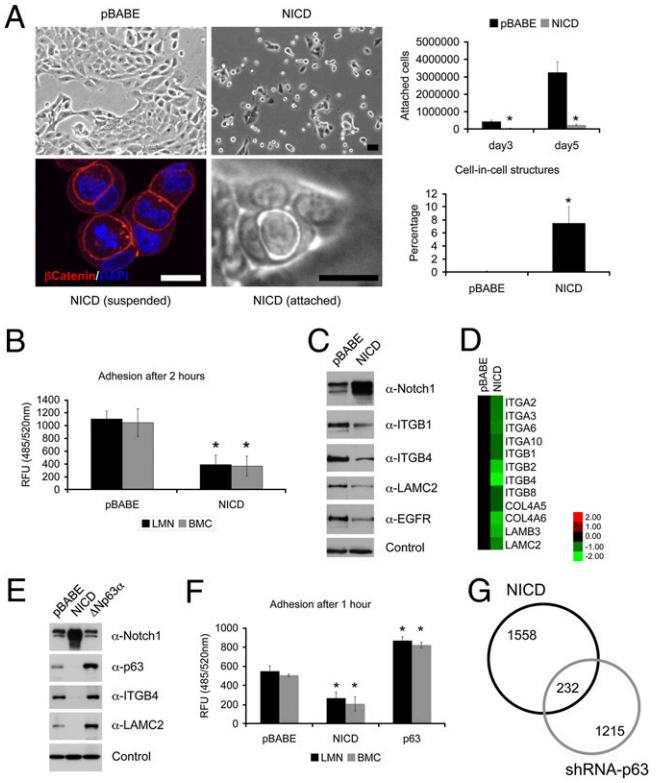

Fig. 2. NICD induces cell-to-matrix detachment. (*A*) Evidence of cell detachment and cell-in-cell structures in MCF-10A cells overexpressing NICD. (*Upper*) Representative phase-contrast images of MCF-10A cells stably infected with control (pBABE) or NICD-encoding retroviral vectors 48 h after replating. These cells also were seeded on day 0 in triplicate at 10×10^3 per well in six-well plates in growth medium. Attached cells then were trypsinized and counted with a hemacytometer on days 3 and 5. Error bars show ± SD of three replicate samples from one representative experiment. *, $P < 0.001$ relative to control. (*Lower*) The confocal image shows representative cell-in-cell structures induced by NICD in suspension and stained for βcatenin (red) and DAPI (blue). The phase-contrast image shows a representative cell-in-cell structure induced by NICD in attached cell monolayers. The percentage of similar structures also was determined by manual counting with a 100× objective. Error bars show ± SD of three replicate samples from one representative experiment. At least five fields were counted for sample. *, $P < 0.005$ relative to control. (Scale bars, 20 μm.) (*B*) Quantitation of the effect of NICD overexpression on cell adhesion to extracellular matrix. Cells infected with the indicated viral vectors were plated on dishes coated with mouse laminin-1 or basement membrane components for 2 h, and adherent cells were quantified following 1-h incubation with calcein acetoxymethyl ester at 37 °C. Fluorescence was measured at 485–520 nm. Values represent the mean ± SD of three replicate samples from one representative experiment. *, $P < 0.01$ relative to control. (*C*) Down-regulation of matrix-to-cell adhesion proteins by NICD. Lysates derived from MCF-10A cells infected with pBABE or NICD retroviruses were analyzed by Western blotting with the indicated antibodies. (*D*) The heat map shows down-regulation of integrins and ECM components by NICD at the transcriptional level. Gene-expression profiling of MCF-10A cells infected with pBABE (control) or NICD retroviruses was performed in triplicate. These data were analyzed as described in *SI Material and Methods*. (*E*) MCF-10A cells infected with the indicated retroviral vectors were analyzed by Western blotting with the indicated antibodies. (*F*) The same cell lines as in E were plated on dishes coated with mouse laminin-1 or basement membrane components for 1 h; then adherent cells were quantified as described above. Values represent the mean ± SD of three replicate samples from one representative experiment. *, $P < 0.001$ relative to control. (*G*) Comparative analysis of microarray data generated from analysis of control and NICD-expressing MCF-10A cells or from control and p63–down-regulated MCF-10A cells (20).

CELL BIOLOGY

exogenous matrix proteins (e.g., mouse laminin-1 or reconstituted basement membrane components) (Fig. 2*B*). The cell-to-matrix detachment triggered by NICD overexpression is associated with a reduction in the levels of expression of integrin β1 (ITGB1) and integrin β4 (ITGB4) as well as the basement membrane component laminin γ2 (LAMC2), a subunit of laminin 332 (also referred to as "laminin 5") (Fig. 2*C*). In addition, we found that mRNAs encoding multiple integrins and matrix proteins expressed in MCF-10A cells are significantly [false-discovery rate (FDR)-adjusted $P < 0.01$] down-regulated in cells expressing NICD (Fig. 2*D* and Dataset S1).

Of note, we also detected a marked reduction in expression levels of EGF receptor (EGFR) (Fig. 2*C*), an effect we previously reported as accompanying loss of integrin engagement in MCF-10A and other epithelial cells (20). Taken together, NICD-induced loss of matrix-to-cell adhesion, formation of cell-in-cell structures, and reduction in EGFR could contribute to suppress the outgrowth of acinar structures in 3D cultures of mammary epithelial cells.

Inverse Regulation of Matrix Adhesion by Notch and p63. The matrix-detachment phenotype induced by NICD strongly resembles the phenotype induced by p63 down-regulation that we reported previously (20). Notch has been shown to down-regulate p63 in keratinocytes (21, 22), raising the possibility that Notch may induce cell detachment in mammary epithelial cells through down-regulation of p63. We found that NICD expression induced down-regulation of p63 mRNA (fold change −2.18, FDR-adjusted $P = 1.85 \times 10^{-7}$; Dataset S1). Furthermore, NICD also suppresses p63 protein expression, correlating with ITGB4 and LAMC2 down-regulation (Fig. 2*E*). Conversely, overexpression of ΔNp63α, the predominant isoform expressed in MCF-10A and other epithelial cells, induces expression of ITGB4 and LAMC2 and increases matrix adhesion (Fig. 2 *E* and *F*).

Because NICD overexpression in MCF-10A cells caused a loss of cell adhesion similar to that induced by down-regulation of p63 with an shRNA targeting the DNA binding domain of all six p63 isoforms (20), we looked for genes that were similarly regulated by NICD overexpression and p63 down-regulation in our microarray studies. The extent of overlap (232 genes) was significantly greater than expected by chance ($P = 0.0034$, Fisher's exact test) (Fig. 2*G* and Dataset S2). Fifteen of these genes (including integrins *ITGA2*, *ITGA6*, *ITGA10*, *ITGB1*, and *ITGB4* and laminins *LAMB3* and *LAMC2*; Dataset S2) have been implicated in cell–matrix interactions based on GeneGO analysis. This value represents a highly significant enrichment in the Cell adhesion_Cell-matrix interaction GeneGO category (15 of 232 versus 166 of 13,106; $P = 7.150^{-5}$). Thirty-six of the genes similarly regulated by NICD overexpression and p63 down-regulation showed the opposite effect in the microarrays of cells overexpressing ΔNp63α (20), further supporting an inverse relationship between genes regulated by NICD and ΔNp63α (Fig. S1 and Dataset S3). Seven of these genes have been implicated in cell–matrix adhesion, and eight are cytoskeletal proteins. Taken together, our data indicate that cell-to-matrix adhesion is inversely regulated by ΔNp63α and NICD and that ΔNp63α down-regulation is likely to contribute, at least in part, to NICD-induced matrix-to-cell detachment.

NICD-Induced Hyperproliferative Response Requires STAT3 Activation. To identify down-stream regulators of Notch pathway activation in mammary epithelial cells, we performed reverse-phase protein array (RPPA) analysis to probe the expression or phosphorylation state of 46 proteins, many of which are altered in oncogene- and growth factor-activated cells (23). Protein fractions were isolated from MCF-10A cells 48 h postinfection with pBABE or NICD retroviral vectors. Phosphorylation of T180/Y182 of p38 increased 2.8-fold, total Src levels increased 2.4-fold, and there also was a 2.4-fold increase in the level of cyclin D1. Of note, there was no increase in phosphorylation of proteins in either the PI3K-AKT or ERK pathway. Surprisingly, we found that the most prominent alteration in NICD-expressing cells was a more than 13-fold increase in phosphorylation (Tyr705) of STAT3 (Fig. 3*A*). This last finding was verified by Western blot analysis (Fig. 3 *B* and *C*).

To address whether JAK kinases are required for STAT3 phosphorylation or any NICD-induced phenotypes, we treated NICD-overexpressing cells with the pan-JAK inhibitor P6. P6 has been shown to have low toxicity in MCF-10A cells and to inhibit JAK/STAT3 signaling with higher sensitivity and specificity than the tyrphostin AG490 (24). P6 inhibited STAT3 phosphorylation as well as the outgrowth of NICD-induced hyperproliferative structures in reconstituted basement membrane gels (Fig. 3 *B* and *D*). Similar results were obtained by down-regulation of STAT3 using a previously characterized lentiviral vector, S3SH, encoding an shRNA targeting STAT3 (24) (Fig. 3 *C*–*E*). Interestingly, the inhibition of STAT3 phosphorylation by P6 or STAT3 shRNA down-regulation did not affect NICD-induced down-regulation of p63 and matrix-

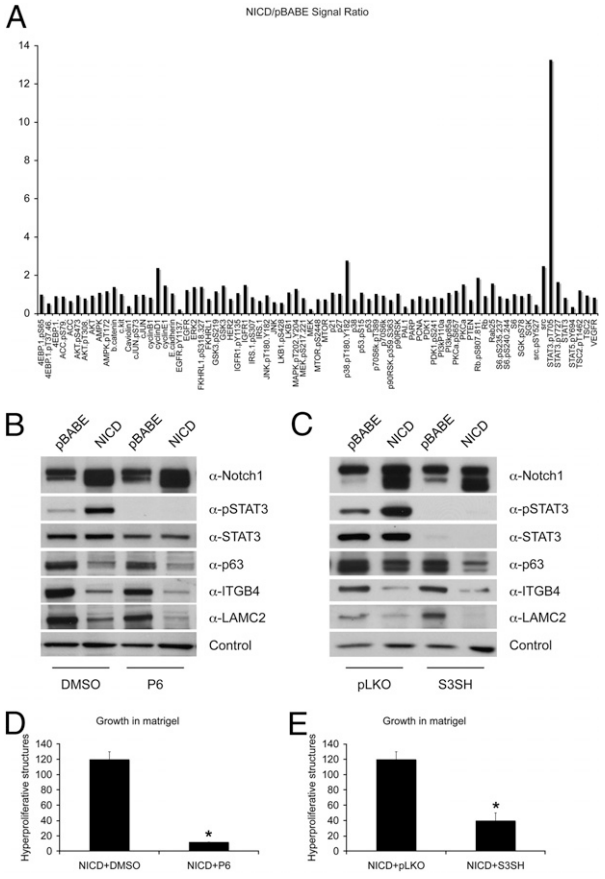

Fig. 3. NICD-induced hyperproliferative response requires STAT3 activation. (*A*) RPPA profile of MCF-10A cells 48 h after infection with pBABE or NICD. Values represent the ratios (NICD/pBABE) of one experiment (three replicate samples). (*B* and *C*) STAT3 inhibition does not affect the NICD-induced down-regulation of p63 and ECM components. The indicated cell lines were analyzed by Western blotting with the indicated antibodies. Where indicated, the cell lines were treated with the pan-JAK inhibitor P6 (1 μM) (Calbiochem) or infected with S3SH, an shRNA lentivirus targeting STAT3 mRNA. (*D* and *E*) STAT3 inhibition affects the outgrowth of hyperproliferative structures induced by NICD in MCF-10A cells. Cells infected with retroviral vectors encoding the indicated genes were grown in Matrigel for 2 weeks. Where indicated, the cultures were fed with P6 once a week. Data show the mean number of hyperproliferative acinar structures (defined as structures larger than control 3D acinar structures) per eight-chamber culture of 6,000 cells. Error bars show ± SD of three replicate samples from one representative experiment. The total number of structures per chamber was counted. *, $P < 0.001$ (*D*) or <0.005 (*E*).

adhesion proteins (Fig. 3 *B* and *C*). These data provide evidence that the JAK/STAT3 pathway is required for the NICD-induced outgrowth of acinar structures in 3D cultures but is not involved with the NICD-dependent effects on matrix-adhesion genes.

Dose-Dependent Regulation of the Heterogeneous Phenotypes Induced by Notch Pathway Activation. The heterogeneous phenotypic responses to NICD overexpression in 3D cultures could reflect quantitative differences in Notch pathway activation levels. To address this possibility, we used a bicistronic vector that coexpresses GFP and NICD to assess the level of NICD expression in the different types of NICD-induced 3D structures. Prior studies using this vector have shown that GFP expression correlates with levels of NICD expression (25). We found striking differences in the levels of GFP expression in the two different types of 3D structures induced by NICD (Fig. 4). In particular, the abortive structures contained significantly more intense GFP fluorescence than the large hyperproliferative structures, thus suggesting an inverse correlation between the level of NICD expression and the extent of clonal outgrowth. Quite notably, the abortive structures failed to show detectable levels by immunostaining for two matrix-adhesion proteins (ITGB1 and LAMC2) expressed in 3D cultures of MCF-10A cells, suggesting that high levels of NICD suppress the expression of these matrix-adhesion proteins (white arrows in Fig. 4). Consistent with this suggestion, the large hyperproliferative structures retained ITGB1 or LAMC2 expression (Fig. 4). These results indicate that high-dose NICD is associated with loss of matrix-adhesion proteins, formation of abortive structures, and limited outgrowth, whereas low-dose NICD is associated with maintenance of matrix proteins and hyperproliferation of 3D structures.

To address dose-dependent effects further, we induced Notch pathway activation at lower levels in the whole cell population using a weak gain-of-function variant of Notch-1, L1601P+ΔP, expressed from the same bicistronic internal ribosome entry site (IRES)-GFP vector described above. This oncogenic variant, originally found in human T-cell acute lymphoblastic leukemia, elicits a ligand-independent activation of the Notch receptor that is weaker than the activity associated with the expression of NICD (26). We corroborated this activity in 293T cells by examining a Notch-dependent luciferase reporter containing the transcription factor CSL binding site: L1601P+ΔP expressed 3-fold lower luciferase activity than NICD and about 2-fold higher luciferase activity than wild-type Notch-1 (Fig. S2*A*). In addition, we analyzed the gene-expression profiles induced 48 h after infection of MCF-10A cells with retroviral vectors expressing full-length Notch-1, L1601P+ΔP, or NICD (Fig. 5*A*). Although expression of each Notch-1 receptor variant was similar in all transduced cell populations (see NOTCH1 in Fig. 5*A*), we detected a dose-dependent

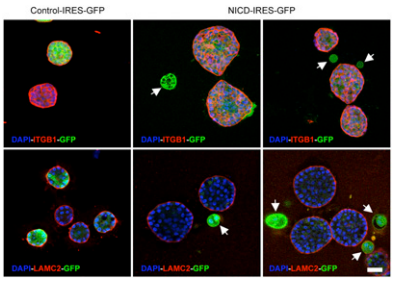

Fig. 4. The heterogeneous phenotypes induced by Notch in 3D reflect differences in the expression levels of NICD-IRES-GFP and cell–matrix adhesion genes. Representative confocal images of 3D structures induced by control-IRES-GFP and NICD-IRES-GFP vectors after 2 weeks. (*Upper*) ITGB1 (red), GFP (green), and DAPI (blue); (*Lower*) LAMC2 (red), GFP (green), and DAPI (blue). The arrows indicate the presence of abortive structures. Of note, control-IRES-GFP induces normal acinar structures independent of GFP expression levels. (Scale bars, 100 μm.)

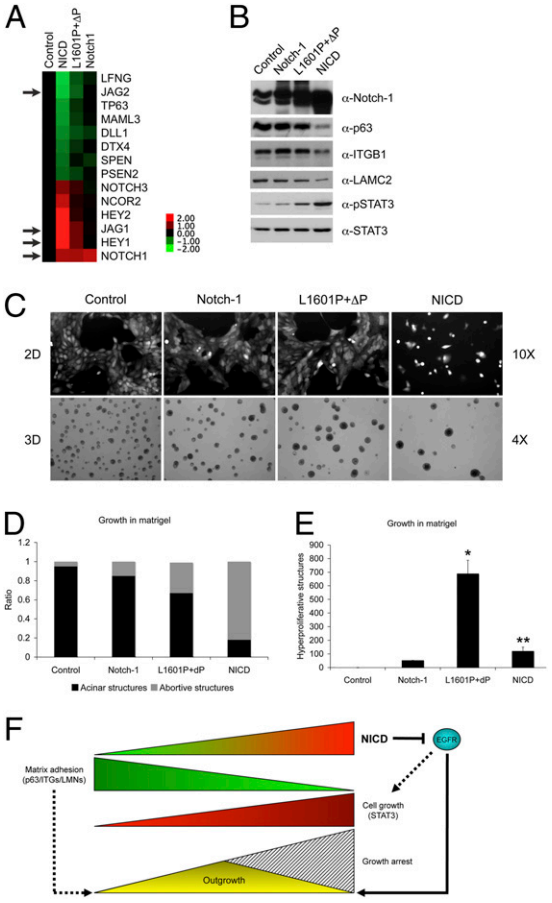

Fig. 5. Dose-dependent regulation of the heterogeneous phenotypes induced by Notch pathway activation. (*A*) The transcriptional changes in genes from the Notch signaling pathway GeneGO category were analyzed as described in *SI Material and Methods*. The black arrows indicate that JAG2, JAG1, and HEY1 are significantly affected by L1601P+ΔP at this threshold (FDR-corrected $P < 0.05$; fold change >1.5). (*B*) MCF-10A cells expressing wild-type Notch-1, L1601P+ΔP mutant, and NICD were sorted by FACS; cell populations expressing similar levels of GFP were isolated and analyzed by Western blotting with the indicated antibodies. (*C*) Heterogeneous phenotypes induced by different variants of Notch-1 receptor. Representative images of the cellular phenotypes induced in 2D and 3D cultures are shown for each cell line. (*D*) The ratio between the number of acinar structures (defined as structures at least as large as controls) and the number of abortive structures relative to the total number of structures was determined by manual counting. (*E*) Data were obtained as the mean number of hyperproliferative acinar structures (defined as structures larger than control acinar structures) developed after 2 weeks in Matrigel. Error bars show SD of three replicate samples from one representative experiment. *, $P < 0.001$ and **, $P < 0.005$ relative to Notch-1. (*F*) Proposed dose-dependent model for Notch pathway involvement in the control of clonal outgrowth of mammary epithelial cells.

induction of several Notch target genes (e.g., *HEY1*, *HEY2*) (Fig. 5*A*) as well as regulation of other relevant genes (e.g., integrins, ECM components, and STAT3 targets; Fig. S3). Full-length Notch-1 induced the weakest effect, with only four genes regulated (*PLA2G2A*, *OLFM4*, and *NOTCH1* up-regulated; RAP1A down-regulated) at levels 1.5-fold or greater than control cells (FDR-adjusted $P < 0.05$). L1601P+ΔP induced an intermediate effect with 192 differentially expressed genes (147 up-regulated, 45 down-regulated) (Dataset S4), and NICD caused transcriptional changes in 1,790 genes (795 up-regulated, 995 down-regulated) (Dataset S1). Importantly, except for one gene, all genes induced by Notch-1 and L1601P+Δ also were altered significantly by NICD (FDR-adjusted $P < 0.05$,

CELL BIOLOGY

>1.35-fold), indicating that there are no unique gene programs induced by full-length or L1601P+ΔP Notch variants that are not also induced by NICD. Fig. S3 gives a more complete analysis of these array data.

To compare the phenotypic alterations induced by the Notch-1 receptor variants, MCF-10A cells expressing wild-type Notch-1, L1601P+ΔP, and NICD were sorted by FACS, and cell populations expressing similar levels of GFP (see 2D panels in Fig. 5*C*) were isolated and analyzed for expression of relevant proteins, loss of adhesion, acinar formation, and growth in soft agar. Compared with NICD, L1601P+ΔP expression did not suppress endogenous p63, ITGB1, or LAMC2 significantly and induced a lower level of phospho-STAT3 (Fig. 5*B*). Unlike NICD, L1601P+ΔP expression did not cause cell detachment (see 2D panels in Fig. 5*C*), indicating that low-dose Notch activity is not sufficient to suppress matrix adhesion. Moreover, although there was a dose-dependent decrease in the proportion of acinar structures (see 3D panels in Fig. 5 *C* and *D*) as well as a dose-dependent increase in the proportion of growth-inhibited abortive structures induced by the three Notch-1 variants (Fig. 5*D*), the number of hyperproliferative structures did not correlate with the dose of Notch activity. In fact, overexpression of full-length Notch-1 caused only a small number of hyperproliferative 3D structures; however, quite remarkably, L1601P+ΔP induced a dramatic increase in such structures, 6-fold greater than the high-activity NICD variant (Fig. 5*E*). In addition, L1601P+ΔP showed a 10-fold greater activity than NICD in a more traditional transformation assay of colony formation in soft agar (Fig. S2*B*). These results further support the ideas that lower levels of Notch pathway activation sustain matrix-to-cell adhesion and induce outgrowth of hyperproliferative structures and that high-dose Notch activity suppresses matrix adhesion and outgrowth.

To explore more specifically the dose-dependent effects of Notch on cell proliferation per se, we examined cell-cycle progression using time-lapse video microscopy of MCF-10A cells expressing the above-described Notch variants that induce different levels of pathway activation. Cell-cycle progression was monitored using a red fluorescent mCherry fusion protein of geminin, which is absent during the G1 phase and accumulates through the S, G2, and M phases of the cell cycle (27). Geminin levels drop at the metaphase–anaphase transition of mitosis when it is degraded by the anaphase-promoting complex. MCF-10A cells stably expressing mCherry-geminin were monitored for S phase reentry by time-lapse video microscopy from 24 to 72 h after infection with retroviral vectors expressing full-length Notch-1, L1601P+ΔP, or NICD (Video S1, Video S2, Video S3, and Video S4). Activation of Notch pathway at high dose by NICD suppressed reentry of cells into S phase (32% reentry relative to control), whereas expression of full-length Notch-1 or L1601P+ΔP had a more moderate effect (71% and 88% reentry, respectively, relative to control).

Taken together, our data indicate that high-dose NICD can affect cell growth directly and suggest that this inhibitory effect, in addition to loss of matrix adhesion, contributes to the suppression of clonal outgrowth induced by increased Notch activity in 3D cultures of MCF-10A cells (Fig. 5*F*).

Discussion

Our data show that constitutive activation of the Notch pathway induces distinct dose-dependent phenotypic responses. In particular, high levels of Notch pathway activation result in suppression of cell proliferation and clonal outgrowth, down-regulation of multiple matrix-adhesion molecules, dramatic loss of matrix adhesion, and formation of cell-in-cell structures, which we previously demonstrated is triggered by loss of ECM attachment to integrin receptors (16, 17). In contrast, lower levels of Notch-1 activity maintain matrix adhesion and induce a proliferative response associated with the outgrowth of acinar structures in 3D cultures and colonies in soft agar. Here, we propose a model to explain the dose-dependent heterogeneous responses to Notch pathway activation (Fig. 5*F*). At low doses, Notch-induced proliferative signals would dominate, and integrins expression would be retained; at higher doses, the deadhesion and growth arrest/differentiation programs would dominate, down-regulating expression of p63, integrins, and matrix proteins, inhibiting outgrowth, and promoting luminal differentiation.

Our studies also highlight a major role for two pathways in the Notch-induced hyperproliferative response: the EGFR and JAK-STAT3 pathways. This idea is based on evidence that EGF-depleted medium failed to support proliferation of NICD-expressing MCF-10A cells and that inhibition of either JAK or STAT3 prevented outgrowth. The basis for the suppression of cell proliferation and clonal outgrowth by high-dose Notch activation probably is mediated by multiple effectors. (*i*) Loss of matrix adhesion could influence cell proliferation significantly, because epithelial cells require matrix adhesion for effective transduction of signals from growth factor receptor stimulation (28). (*ii*) The formation of cell-in-cell structures (through entosis) induced by loss of adhesion also would limit clonal outgrowth because internalized cells typically undergo lysosomal destruction (16, 17). (*iii*) The dramatic down-regulation of EGFR protein and mRNA expression by NICD also would limit the proliferative capacity of cells (Fig. 2*C* and Dataset S1). We have shown previously that EGFR is down-regulated dramatically following detachment from matrix (29); thus, loss of EGFR could be a secondary consequence of lack of integrin engagement. However, down-regulation of p63 by high-dose NICD also could contribute to EGFR repression, because loss of p63 has been shown to reduce EGFR mRNA expression (20). (*iv*) Multiple EGFR ligands (AREG, AREGB, HB-EGF; Dataset S1) also are down-regulated by NICD. (*v*) There is a dose-dependent induction of the cyclin CDK inhibitor p21, which previously was shown to be required for NICD-induced growth arrest in different types of epithelial cells (30, 31) (Fig. S4*A*). Of note, we found that over-expression of NICD in $p21^{-/-}$ MCF-10A cells did not significantly rescue the suppression of clonal outgrowth in the 3D model employed here (Fig. S4*B*). Given the broad range of NICD-induced gene alterations affecting both cell proliferation and matrix adhesion (which is known to be required for cell proliferation in many contexts), it is likely that reversing the effects of NICD on any one gene will not alone rescue the suppression of clonal outgrowth.

Interestingly, high-dose NICD did not prevent activation of the JAK-STAT pathway. STAT3 phosphorylation correlated positively with Notch activation levels, showing increased phosphorylation at elevated levels of Notch pathway activation (Fig. 5*B*). STAT3 is constitutively activated in more than 50% of primary breast tumors and tumor-derived cell lines. Recently, it has been shown that direct protein–protein interactions can coordinate cross-talk between the Notch-Hes and JAK-STAT pathways (32). Our data indicate that the JAK/STAT pathway is required for outgrowth of hyperproliferative structures induced by NICD but is not involved with the NICD-dependent effects on matrix adhesion (Fig. 3). Thus, the deadhesion program is independent of the JAK-STAT3 pathway, and the outgrowth failure at high-dose NICD does not involve suppression of STAT3 activation.

Recently, Notch-1 also was shown to promote commitment of mouse mammary stem cells (MaSCs) exclusively along the luminal lineage (33), and Notch-3 was shown to be required for differentiation of bipotent progenitor cells into luminal progenitors (34). Differentiation into luminal cells is associated with loss of p63 and reduction in expression of basal integrins and matrix proteins. Thus, the p63 down-regulation induced at high dose in NICD-expressing MCF-10A cells also would be consistent with a Notch-dependent luminal differentiation program. Interestingly, our analysis of NICD-regulated genes in MaSC-enriched, luminal progenitor, and mature luminal cell gene sets (35) suggests that Notch suppression of p63 may be responsible for the down-regulation of multiple integrins and matrix proteins in luminal progenitor cells, because these cells are distinguished from MaSCs by low levels of p63 and NICD-regulated matrix-adhesion proteins (Fig. S5). High-dose NICD also could collaborate with other differentiation factors to suppress pro-

liferation during terminal differentiation in vivo. It is possible that Notch limits expansion of MaSCs, because knockdown of the canonical Notch effector centromere binding protein 1 (CBF-1) in the MaSC-enriched population was reported to elevate stem cell activity in vivo as well as the formation of aberrant end buds in mice; and inhibition of Notch signaling using a gamma-secretase inhibitor increased the size of MaSC-enriched colonies in vitro significantly (33). Also, in an earlier study, basal cell proliferation was elevated during pregnancy in mice with targeted CBF-1 disruption (36). These results suggest a role for endogenous Notch signaling in restricting MaSC expansion. Although Notch-1 may not be the active Notch receptor in these cells, NICD overexpression may have promiscuous activities on other Notch family targets.

In summary, our data have revealed mechanisms whereby phenotypic responses to Notch are influenced by dose-dependent effects on cell adhesion and growth in mammary epithelial cells. Dose-dependent effects of Notch have been observed in other contexts as well. Studies in *Drosophila melanogaster* have revealed that cells expressing different levels of Notch can regulate distinct cell-cycle mediators, suggesting that a dose-dependent mechanism could contribute to growth regulation in this organism (37). In addition, in cervical cells, high-dose NICD suppresses expression of the human papilloma viral oncogene E6 and E7, whereas at moderate doses NICD collaborates with E6 and E7 to transform primary cells (38). Notch control of both proliferation and differentiation also resembles the dichotomous dose-dependent activities of Myc on these two phenotypes in epidermal cells (39). It is likely that the level and duration of Notch activation within the mammary gland differentially affects mammary cell growth and adhesion. In addition, our data also suggest that during the evolution of epithelial tumors triggered by Notch pathway activation, there would be a selection for cells expressing lower levels of Notch pathway activation because these cells would have the greatest proliferative potential. It is clearly of great interest to determine which factors affect the level of Notch pathway function and to explore further the basis for dose-dependent effects during distinct phases of development and tumorigenesis.

Materials and Methods

Details of the procedures and microarray analysis are described in *SI Text*. Assays were conducted with three replicate samples in at least two independent experiments. Statistical analyses were performed using unpaired Student's *t* test. Raw and processed microarray data can be accessed at the Gene Expression Omnibus (www.ncbi.nlm.nih.gov/geo, GSE20285 and GSE20286).

ACKNOWLEDGMENTS. We thank Qiang Sun for providing an image of NICD-induced invading cells, Christopher Winter, Heike Keilhack, Pamela Carroll, and Stephan Krauss for helpful comments on the project, Jackie Bromberg (Memorial Sloan-Kettering Cancer Center, New York) for generously providing the Stat3 shRNA vector; Atsushi Miyawaki (Brain Science Institute, Hirosawa, Japan) for providing the mCherry-geminin reporter, and Ben Ho Park (The Johns Hopkins University, Baltimore, MD) for the p21-knocked out MCF-10A cells. We also thank Senthil Muthuswamy (Ontario Cancer Institute, Toronto) for helpful comments on the manuscript and members of the Brugge laboratory for fruitful discussions. In addition we are grateful for a gift from Lee Jeans through the Entertainment Industry Foundation (J.S.B.). This work also was supported by Grants R01 CA098402 and R37 NS26084 from the Leukemia and Lymphoma Society (to S.A.-T.); Grants P01 CA119070 (to J.C.A.), P01 CA099031 (to G.B.M.), and P01 CA105134 (to J.S.B.) from the National Cancer Institute; Grant P30CA16672 from Cancer Center Support Grant (to G.B.M.); and a grant from Merck Research Laboratories Boston (to J.S.B.). M.M. was a recipient of the L. Fontana e M. Lionello fellowship from the Associazione Italiana per la Ricerca sul Cancro. J.A. is supported by a multidisciplinary postdoctoral fellowship from the U.S. Army Breast Cancer Research Program.

1. Artavanis-Tsakonas S, Matsuno K, Fortini ME (1995) Notch signaling. *Science* 268: 225–232.
2. Artavanis-Tsakonas S, Rand MD, Lake RJ (1999) Notch signaling: Cell fate control and signal integration in development. *Science* 284:770–776.
3. Radtke F, Raj K (2003) The role of Notch in tumorigenesis: Oncogene or tumour suppressor? *Nat Rev Cancer* 3:756–767.
4. Rizzo P, et al. (2008) Rational targeting of Notch signaling in cancer. *Oncogene* 27: 5124–5131.
5. Weng AP, et al. (2004) Activating mutations of NOTCH1 in human T cell acute lymphoblastic leukemia. *Science* 306:269–271.
6. Pece S, et al. (2004) Loss of negative regulation by Numb over Notch is relevant to human breast carcinogenesis. *J Cell Biol* 167:215–221.
7. Reedijk M, et al. (2005) High-level coexpression of JAG1 and NOTCH1 is observed in human breast cancer and is associated with poor overall survival. *Cancer Res* 65: 8530–8537.
8. Stylianou S, Clarke RB, Brennan K (2006) Aberrant activation of notch signaling in human breast cancer. *Cancer Res* 66:1517–1525.
9. Gallahan D, et al. (1996) Expression of a truncated Int3 gene in developing secretory mammary epithelium specifically retards lobular differentiation resulting in tumorigenesis. *Cancer Res* 56:1775–1785.
10. Kiaris H, et al. (2004) Modulation of notch signaling elicits signature tumors and inhibits hras1-induced oncogenesis in the mouse mammary epithelium. *Am J Pathol* 165:695–705.
11. Capobianco AJ, Zagouras P, Blaumueller CM, Artavanis-Tsakonas S, Bishop JM (1997) Neoplastic transformation by truncated alleles of human NOTCH1/TAN1 and NOTCH2. *Mol Cell Biol* 17:6265–6273.
12. Raafat A, Bargo S, Anver MR, Callahan R (2004) Mammary development and tumorigenesis in mice expressing a truncated human Notch4/Int3 intracellular domain (h-Int3sh). *Oncogene* 23:9401–9407.
13. Weaver VM, Bissell MJ (1999) Functional culture models to study mechanisms governing apoptosis in normal and malignant mammary epithelial cells. *J Mammary Gland Biol Neoplasia* 4:193–201.
14. Debnath J, Brugge JS (2005) Modelling glandular epithelial cancers in three-dimensional cultures. *Nat Rev Cancer* 5:675–688.
15. Debnath J, et al. (2002) The role of apoptosis in creating and maintaining luminal space within normal and oncogene-expressing mammary acini. *Cell* 111:29–40.
16. Overholtzer M, et al. (2007) A nonapoptotic cell death process, entosis, that occurs by cell-in-cell invasion. *Cell* 131:966–979.
17. Overholtzer M, Brugge JS (2008) The cell biology of cell-in-cell structures. *Nat Rev Mol Cell Biol* 9:796–809.
18. Ayyanan A, et al. (2006) Increased Wnt signaling triggers oncogenic conversion of human breast epithelial cells by a Notch-dependent mechanism. *Proc Natl Acad Sci USA* 103:3799–3804.
19. Smith GH, et al. (1995) Constitutive expression of a truncated INT3 gene in mouse mammary epithelium impairs differentiation and functional development. *Cell Growth Differ* 6:563–577.
20. Carroll DK, et al. (2006) p63 regulates an adhesion programme and cell survival in epithelial cells. *Nat Cell Biol* 8:551–561.
21. Nguyen BC, et al. (2006) Cross-regulation between Notch and p63 in keratinocyte commitment to differentiation. *Genes Dev* 20:1028–1042.
22. Okuyama R, et al. (2007) p53 homologue, p51/p63, maintains the immaturity of keratinocyte stem cells by inhibiting Notch1 activity. *Oncogene* 26:4478–4488.
23. Tibes R, et al. (2006) Reverse phase protein array: Validation of a novel proteomic technology and utility for analysis of primary leukemia specimens and hematopoietic stem cells. *Mol Cancer Ther* 5:2512–2521.
24. Berishaj M, et al. (2007) Stat3 is tyrosine-phosphorylated through the interleukin-6/glycoprotein 130/Janus kinase pathway in breast cancer. *Breast Cancer Res* 9:R32.
25. Pui JC, et al. (1999) Notch1 expression in early lymphopoiesis influences B versus T lineage determination. *Immunity* 11:299–308.
26. Chiang MY, et al. (2008) Leukemia-associated NOTCH1 alleles are weak tumor initiators but accelerate K-ras-initiated leukemia. *J Clin Invest* 118:3181–3194.
27. McGarry TJ, Kirschner MW (1998) Geminin, an inhibitor of DNA replication, is degraded during mitosis. *Cell* 93:1043–1053.
28. Miranti CK, Brugge JS (2002) Sensing the environment: A historical perspective on integrin signal transduction. *Nat Cell Biol* 4:E83–E90.
29. Reginato MJ, et al. (2003) Integrins and EGFR coordinately regulate the pro-apoptotic protein Bim to prevent anoikis. *Nat Cell Biol* 5:733–740.
30. Rangarajan A, et al. (2001) Notch signaling is a direct determinant of keratinocyte growth arrest and entry into differentiation. *EMBO J* 20:3427–3436.
31. Niimi H, Pardali K, Vanlandewijck M, Heldin CH, Moustakas A (2007) Notch signaling is necessary for epithelial growth arrest by TGF-beta. *J Cell Biol* 176:695–707.
32. Kamakura S, et al. (2004) Hes binding to STAT3 mediates crosstalk between Notch and JAK-STAT signalling. *Nat Cell Biol* 6:547–554.
33. Bouras T, et al. (2008) Notch signaling regulates mammary stem cell function and luminal cell-fate commitment. *Cell Stem Cell* 3:429–441.
34. Raouf A, et al. (2008) Transcriptome analysis of the normal human mammary cell commitment and differentiation process. *Cell Stem Cell* 3:109–118.
35. Lim E, et al.; kConFab (2009) Aberrant luminal progenitors as the candidate target population for basal tumor development in BRCA1 mutation carriers. *Nat Med* 15:907–913.
36. Buono KD, et al. (2006) The canonical Notch/RBP-J signaling pathway controls the balance of cell lineages in mammary epithelium during pregnancy. *Dev Biol* 293:565–580.
37. Price DM, Jin Z, Rabinovitch S, Campbell SD (2002) Ectopic expression of the Drosophila Cdk1 inhibitory kinases, Wee1 and Myt1, interferes with the second mitotic wave and disrupts pattern formation during eye development. *Genetics* 161:721–731.
38. Lathion S, Schaper J, Beard P, Raj K (2003) Notch1 can contribute to viral-induced transformation of primary human keratinocytes. *Cancer Res* 63:8687–8694.
39. Watt FM, Frye M, Benitah SA (2008) MYC in mammalian epidermis: How can an oncogene stimulate differentiation? *Nat Rev Cancer* 8:234–242.